Development of New Drugs to Treat Tuberculosis Based on the Dinitrobenzamide Scaffold

Tiago Delgado , João Pais , David Pires , Filipe Estrada , Rita Guedes , Elsa Anes , Luís Constantino *

Posted Date: 14 March 2024

doi: 10.20944/preprints202403.0811.v1

Keywords: Tuberculosis; DprE1; DNB; TB; Nitrobenzamides

Article

Development of New Drugs to Treat Tuberculosis Based on the Dinitrobenzamide Scaffold

Tiago Delgado [1], João Pais [1,2], David Pires [1,2], Filipe Estrada [1,2], Rita Guedes [1,2], Elsa Anes [1,2] and Luís Constantino [1,2,*]

[1] Research Institute for Medicines and Pharmaceutical Sciences (iMed.UL), Av. Prof. Gama Pinto, 1649-003 Lisboa, Portugal
[2] Faculdade de Farmácia, Universidade de Lisboa, Av. Prof. Gama Pinto, 1649-003 Lisboa, Portugal
* Correspondence: constant@ff.ul.pt

Abstract: Despite the efforts made to stop the tuberculosis (TB) epidemic, it still remains one of the leading causes of death from an infectious disease. Previous work in the group uncovered a new family of amides which showed promising activities against *Mycobacterium tuberculosis*. A closer look at the literature showed that these compounds are structurally related to the DNB family of DprE1 inhibitors, so, we decided to study a wide range of substituted amides and determine their activity, focusing on unexplored structures related to the dinitrobenzamides (DNB) found in the literature. To synthesize our library of compounds we started from 3,5-dinitrobenzoic acid to form the nitroaromatic core that is characteristic of the DNB's, to which we then added linear or cyclic amine moieties. Additionally, the impact of terminal aromatic moieties was also assessed for some derivatives, via an ether, ester, or amide bond. In order to obtain the desired derivatives, multiple synthetic approaches were used, mainly focused on nucleophilic addition/elimination reactions, S_N2 reactions and Mitsunobu reactions. The activity was impacted mainly by two structural features, the addition of an aromatic moiety as a terminal group and the type of the linker. The most interesting compounds exhibited activities comparable to isoniazid and DNB1. Computational studies were also performed aimed at understanding their possible interactions with DprE1. The most active compounds are a good starting point for further development, and we plan to study an extended family of compounds based in those structures.

Keywords: tuberculosis; DprE1; DNB; TB; nitrobenzamides

1. Introduction

Tuberculosis (TB) has afflicted mankind for thousands of years, and, to this day, it still remains one of the leading causes of death from an infectious agent, killing around 1,3 million people every year [1]. TB is usually spread when people who are sick with TB expel bacteria through the air (e.g. by coughing), and only a small number of bacteria are necessary to cause infection [1,2]. A significant problem in the treatment of TB is its prolonged duration and the number of drugs taken concomitantly, since that leads to a lack of drug compliance by the patients and makes monitorization difficult. For the individuals that develop the disease, the current standard treatment of drug-susceptible TB consists of a 6-month drug regimen with the use of 4 different drugs [1]. When drug resistant variants are factored in the therapy becomes even more challenging since require even longer and more aggressive drug regiments [3,4]. The COVID19 pandemic made things even worse and made the "End TB Strategy" goals seem even further away from being achieved, showing that there is an urgent need for more effective drugs against this disease [1].

Mtb has a complex cell wall structure that confers a high degree of impermeability to most drugs due to its hydrophobic character [5]. However, because of its vital role in Mtb survival and the absence of analogous structures in humans, targeting the pathways involved in its synthesis has shown promising results in combating Mtb infections [6,7].

 doi:10.20944/preprints202403.0811.v1

One of the promising targets associated with the cell wall biosynthesis is DprE1, a FAD-dependent oxidoreductase that occupies the periplasm and that is essential for the formation of decaprenyl-phospho-d-arabinofuranose (DPA), the only source of arabinose residues available for the synthesis of the AG layer of the cell wall, and thus essential for the integrity of the cell wall [6].

Several families of compounds can inhibit this enzyme, but they can be mainly divided into 2 groups: the covalent and the non-covalent inhibitors. For the covalent inhibitors, an aromatic nitro group is essential for its mechanism of action. The nitro group is reduced by the FAD cofactor of DprE1, forming a nitroso moiety. Then, the sulfur from a nearby cysteine residue, cysteine 387 (Cys387), attacks the nitroso group, forming a covalent bond between the nitro-aromatic group and the enzyme, permanently inhibiting it [8,9].

The first family of compounds identified as covalent DprE1 inhibitors were the nitrobenzothiazinones (BTZ) [10]. Shortly after, in an independent study, nitrobenzamides were also discovered as covalent inhibitors of DprE1 [11]. This family of compounds can be seen as a simplification of the BTZ structure, as taking the benzothiazinone scaffold and opening the heterocycle ring by removing the sulfur atom (Figure 1).

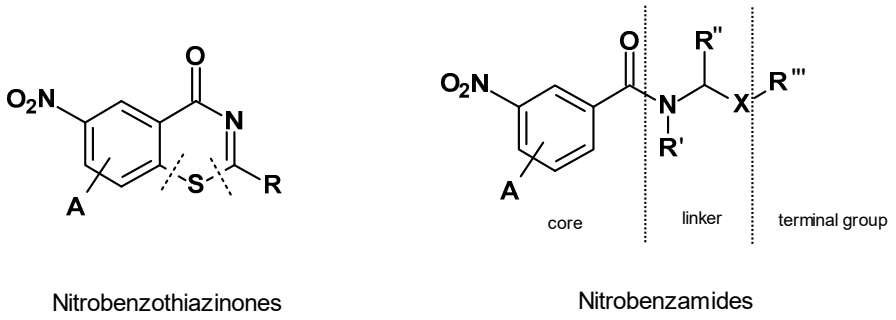

Figure 1. General structure of nitrobenzothiazinones and nitrobenzamides. In this work we focused modifications on the linker and terminal group of dinitrobenzamides (A = 5-NO_2) X = N, CH or O. Some of the nitrobenzamides, such as the family (**a**) developed in this work, have a cyclic linker (R' is connected to X).

Nitrobenzamides as represented in Figure 1 can be broadly divided into three sections: a nitroaromatic benzamide core, containing the nitro group essential for the formation of the covalent bond; a linker, typically comprising a short alkyl structure, a cyclic structure or a combination of both; and a terminal group, commonly an aromatic or aliphatic ring structure. A is generally a second nitro group but can be replaced by another strong electron withdrawing group like a trifluoromethyl. [11–15].

Previous work in our lab uncovered that 3,5-dinitrobenzoic acid esters, and especially its amide isosteres, exhibited promising activities against *M. tuberculosis* [16,17]. A closer look at the literature showed that the compounds were structurally related to the nitrobenzamide family.

Following those results, we decided to study a wide range of substituted amides and determine their activity, focusing on unexplored structures related to the nitrobenzamides. We started by synthesizing a library comprised of 3,5-dinitrobenzamides, varying the type of linker and terminal group present and determined their antitubercular activity. Then we performed computational docking studies and analyzed the position of our compounds within the binding pocket of DprE1, with the objective of trying to further understand how to improve this family of compounds. Three of the nitrobenzamides synthesized were able to have activities comparable to isoniazid and DNB1, and thus are promising leads for future development of this class of inhibitors. The results are reported here.

 doi:10.20944/preprints202403.0811.v1

2. Results

2.1. Compound Library

With the objective of exploring the effect of new modifications to the linker and the terminal group, a library comprised of six different families of 3,5-dinitrobenzamides (**a**-**f**) was obtained (Scheme 1).

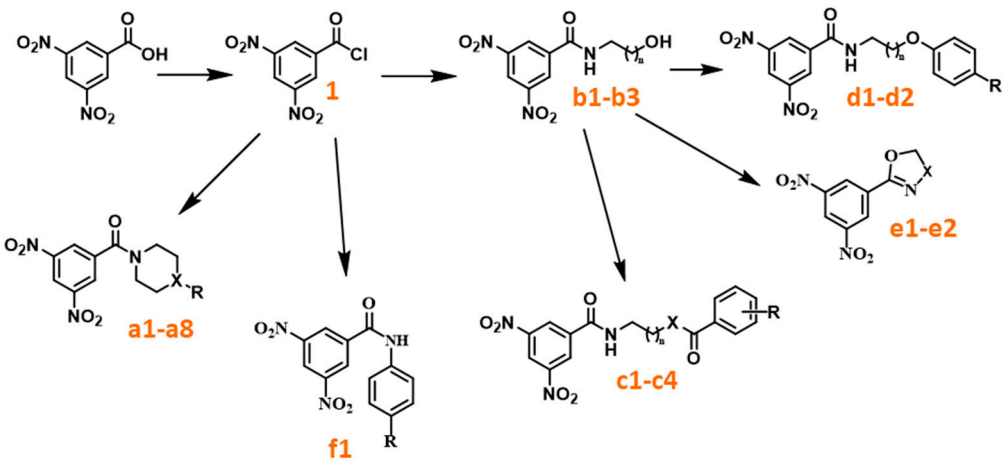

Scheme 1. General scheme of the synthesis of target compounds. Please refer to Table 1 for the structure of individual compounds.

The synthesis of the compounds started from 3,5-dinitrobenzoic acid, which was refluxed in thionyl chloride to originate 3,5-dinitrobenzoyl chloride (**1**). After removing the excess of thionyl chloride by low pressure evaporation, the compound was used without further purification to minimize its degradation. Compound **1** was then coupled with different amines to synthesize compounds **a1**-**a6**, **b1**-**b3**, and **f1** through a nucleophilic addition/elimination reaction, with moderate to good yields (31 to 88%). Compounds **c1** and **c2** were also obtained in a similar manner, but with an inversion the proportions of the amine and compound **1** being used. (3,5-dinitrophenyl)-piperazin-1-yl-methanone (**a2**) was used directly for the formation of compound **a8** by addition of the two methyl groups.

Synthesis of compounds **a7**, **d1** and **d2** was achieved by coupling a 4-methoxyphenol to the terminal hydroxyl group of compounds **a3**, **b2** and **b3** by Mitsunobu reaction [18] (reaction outlined in Scheme 2), with low to moderate yields (29 to 43%).

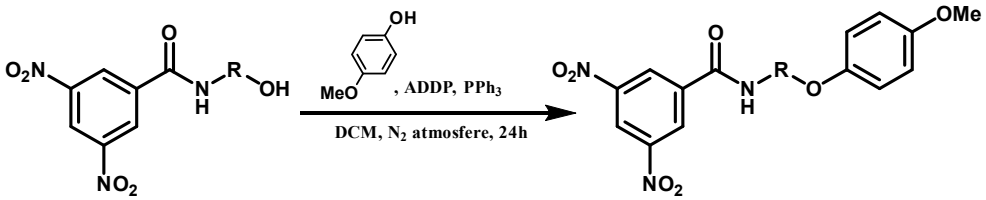

Scheme 2. General step for the Mitsunobu reaction represented for the compounds with linear linkers.

In the case of the reaction using **b1** as the starting material, compound **e1** was produced instead of the expected product. During the reaction there's the formation of an intermediate [18] of starting material coupled with PPh_3. In our case this intermediate likely undergoes an intramolecular reaction (Scheme 3), similar to the one described by Marco Brandstätter et al. [19], since triphenylphosphine oxide (TPPO) is a good leaving group. This reaction had a good yield (70%). Using compound **b2** as a starting material originated compound **e2** as secondary product and compound **d1** as main product.

 doi:10.20944/preprints202403.0811.v1

The mechanism of **e2** formation is likely similar to that of **e1**, however, in this case **d1** was also formed and was the major product. Both compounds were able to be isolated by column chromatography.

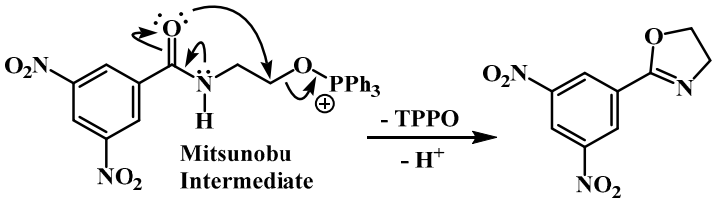

Scheme 3. Possible mechanism for the formation of compound **e1** in the Mitsunobu reaction.

Synthesis of *N*,*N'*-(pentane-1,5-diyl)bis(3,5-dinitrobenzamide) (**c3**) and *N*-(5-benzamidopentyl)-3,5-dinitrobenzamide) (**c4**) required 4 sequential reactions, as outlined in Scheme 4. Compound **b3** was refluxed in a mixture of thionyl chloride and toluene to replace the hydroxyl group by a chloro and originate *N*-(5-chloropentyl)-3,5-dinitrobenzamide (**3**), using DMF as a catalyst. After purification by column chromatography, the compound was obtained with excellent yields (97%). The second step was an S_N2 reaction to replace the 5-chloro group by an azide to obtain *N*-(5-azidopentyl)-3,5-dinitrobenzamide (**4**), with excellent yields (97%). The third step was the transformation of the azide into an amine using PPh_3, via the Staudinger reaction [20]. This compound was used directly in the final step, which consisted of a similar reaction to that of the conjugation of the amines with the acyl chlorides, using either compound **1** or benzoyl chloride (**2**). After purification by column chromatography, the compounds were obtained with low/moderate yields (14 to 55%).

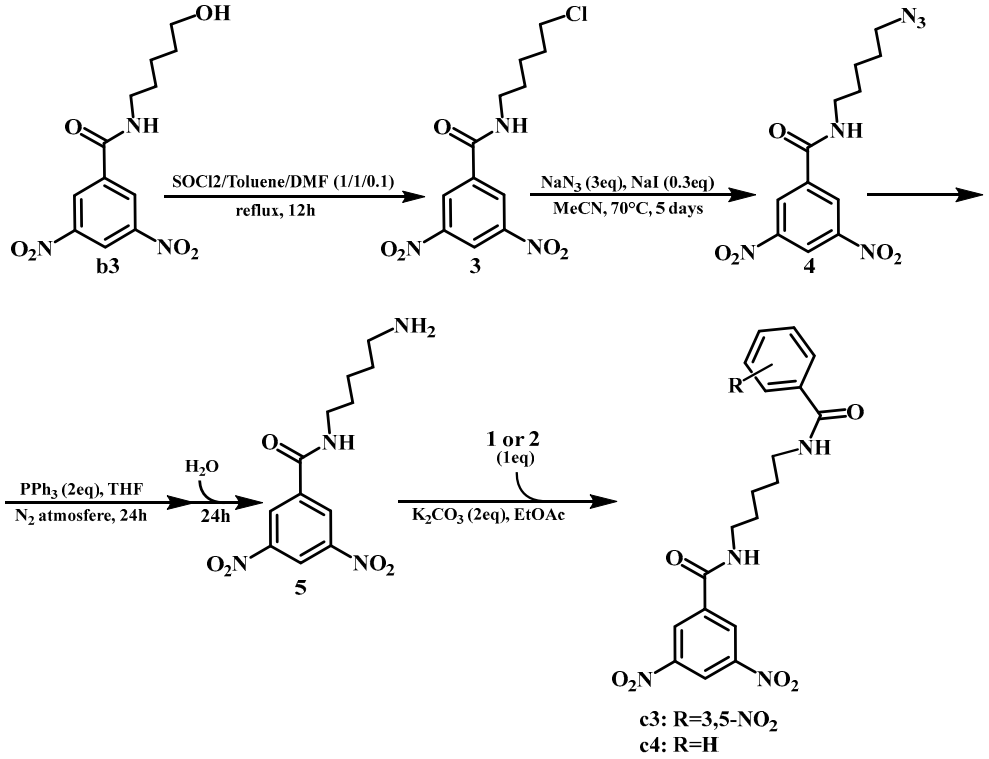

Scheme 4. Synthesis of compounds **c3** and **c4.**

2.2. Antitubercular Activity

The compounds obtained as well as their corresponding antitubercular activity, determined as minimal inhibitory concentration (MIC) and minimal bactericidal concentration (MBC), are presented in Table 1.

 doi:10.20944/preprints202403.0811.v1

Table 1. Library of compounds under study and their corresponding predicted logP values, as well as their antitubercular activity against M. tuberculosis expressed as MIC and MBC values, the mode value of triplicate experiments tested against H37Rv strain of Mtb. Refer to Scheme 2 for the structure of individual compounds.

Compound	R	X	n	Log(P)	MIC (μg/mL)	MBC (μg/mL)
a1	H	CH	-	1.54	>16	>16
a2	-	NH	-	1.33	ND	ND
a3	OH	CH	-	0.77	>16	>16
a4	-	O	-	0.63	>16	>16
a5	Bn	N	-	1.90	2	4
a6	Bn	CH	-	2.95	0.5	2
a7	OPh-(4-OMe)	CH	-	2.50	2	4
a8	Me_2	N	-	-0.31	>16	>16
b1	OH	-	1	0.24	16	-
b2	OH	-	2	0.50	4	16
b3	OH	-	4	1.13	2	4
c1	3,5-NO_2	O	1	1.22	>16	>16
c2	3,5-NO_2	O	4	2.15	0.063	0.25
c3	3,5-NO_2	N	4	1.78	0.25	-
c4	H	N	4	2.45	2	-
d1	OMe	-	2	2.38	0.063	0.125
d2	OMe	-	4	2.93	0.063	0.125
e1	-	-CH_2-	-	0.96	2	4
e2	-	-CH_2CH_2-	-	1.30	16	>16
f1	OMe	-	-	2.00	>16	>16
INH[a]	-	-	-	-	0.063	0.125
DNB1[b]	OMe	-	1	2.04	0.031	0.031

ND (not determined); [a]INH: isoniazid; [b]DNB1 shares a similar structure to the compounds of family **d.**

Table 1 shows that despite the structural variability there are two structural features that may impact activity: the addition of an aromatic moiety as a terminal group and the shape and type of the linker. The addition of an aromatic moiety as a terminal group tends to significantly increase the activities of the compounds. One exception is compound **c1**, where that addition led to a compound with lower activity than compound **b1**. Another important observation is that the linker plays an important role in activity, with compounds that employ linear linkers generally having greater activities than the compounds that have cyclic linkers, and the elimination of the linker (compound **f1**) leading to an inactive compound.

Within the library there's some variation in the lipophilicity of the compounds (from -0,31 to 2.98), however, the most active compounds have LogP values above 2. Figure 2 illustrates the relationship between LogP and antimycobacterial activity for the synthesized compounds.

 doi:10.20944/preprints202403.0811.v1

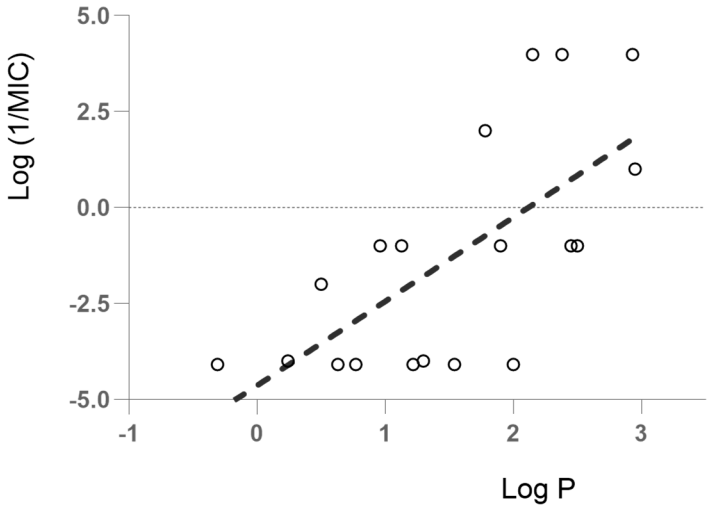

Figure 2. Graphical representation of the correlation between logP and log(MIC) values for the library of compounds. y=2.1898x – 4,6535 R^2= 0.4553.

2.3. Computational Studies

A computational docking study was undertaken to investigate the binding interactions of our compounds within the DprE1 binding site, using the 4FDN PDB structure [21]. During the structure preparation, a water molecule close to the FAD cofactor was preserved due to its pivotal interactions with both the FAD cofactor and the protein. Docking was performed with the GOLD software (Version 2022.1.0) employing the ASP scoring function [22], from which the highest-scoring poses were selected for analysis.

The spatial orientation (poses) of the most active compounds demonstrated proximity to both Cys387 and FAD cofactor. The inhibitors' mechanism of action, requiring the nitro group's activation by $FADH_2$ followed by covalent bonding with Cys387's sulfur, necessitates that the compound enters the active site in a way that positions its nitro group near these critical regions. Thus, the placement of the nitro groups of the most active compounds near these zones is expected (exemplified by compound **d1** in Figure 3A). However, some less active compounds were also found in similar positions, as can be seen in Figure 3B.

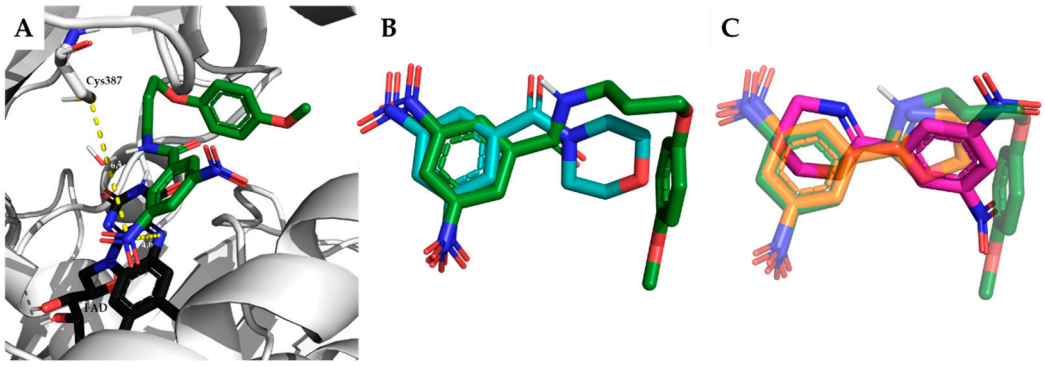

Figure 3. Representation of the best binding poses obtained by docking computational study, between a PDB crystal structure (PDB: 4FDN) and: A - The compound **d1** (green) and the distances between the nitro group and both the cysteine residue (Cys387) and the FAD cofactor (black); B – overlay of compound **a4** (cyan) and compound **d1** (green); C – overlay of compounds **e1** (orange) and **e2** (pink) with compound **d1** (green).

Curiously, half of the compounds exhibiting low activities (>2μg/mL) are oriented inversely within the pocket compared to compound **d1**. An example of this is compound **e2** (illustrated in

 doi:10.20944/preprints202403.0811.v1

Figure 3C), where its 5,6-dihydro-4H-1,3-oxazine ring is positioned similarly to the nitroaromatic core of compound **d1**, albeit with the opposite overall orientation. This stands in contrast to compound **e1** which, despite its structural resemblance to **e2**, assumes a position within the pocket that is more aligned with the orientation of compound **d1**. This observation highlights the nuanced role of molecular orientation in the binding efficacy and activity levels of these compounds.

To conduct a more comprehensive analysis of these findings, we calculated the distances between the nitro groups and two key sites: Cys387 (ND_{Cys387}- which is the distance from the nitrogen atom of the closest nitro group to the sulfur of Cys387) and the FAD cofactor (ND_{FAD} -, the distance from the nitrogen atom of the nearest nitro group to the nitrogen atom in the central portion of the FAD's isoalloxazine ring). These critical distances, along with the docking scores, are detailed in Table 2.

Table 2. Values of the distances obtained from the docking analysis of the best binding poses of the compounds in study and their correspondent scores (kcal/mol) and MIC (μg/mL) values.

Compound	ND_{Cys387}(Å)	ND_{FAD}(Å)	Score (Non-covalent docking)	Score (Covalent docking)	MIC (μg/mL)
a1	4.42	7.63	30.97	20.08	>16
a3	4.49	7.76	32.39	26.93	>16
a4	7.16	5.10	31.17	28.62	>16
a5	6.16	7.75	36.37	23.61	2
a6	6.32	4.51	33.10	25.76	0.5
a7	6.25	4.84	33.06	28.86	2
a8	5.70	4.48	35.60	24.21	>16
b1	5.91	3.94	35.18	30.54	16
b2	6.30	4.44	35.43	28.03	4
b3	6.41	4.36	37.52	31.88	2
c1	5.57	4.61	23.69	17.11	>16
c2	7.62	4.82	26.78	38.33	0.063
c3	5.96	4.62	29.09	37.62	0.25
c4	5.75	4.82	43.45	37.28	2
d1	6.35	4.64	42.43	33.77	0.063
d2	6.33	4.51	42.44	37.25	0.063
e1	6.22	4.37	33.42	27.67	2
e2	4.36	6.73	32.40	28.33	16
f1	5.80	7.42	36.10	7.78	>16

Figure 4 demonstrates the correlation between the distance to FAD and the antitubercular activity. This visualization indicates that there is no clear separation between active and non-active compounds on these metrics. However, an observation from the data suggests that ND_{FAD} values greater than 5.5 Å are commonly found in compounds characterized by lower activity levels. This insight might imply a threshold effect where distances beyond a certain point adversely affect the compound's antitubercular potency.

Preprints.org (www.preprints.org) | NOT PEER-REVIEWED | Posted: 14 March 2024 doi:10.20944/preprints202403.0811.v1

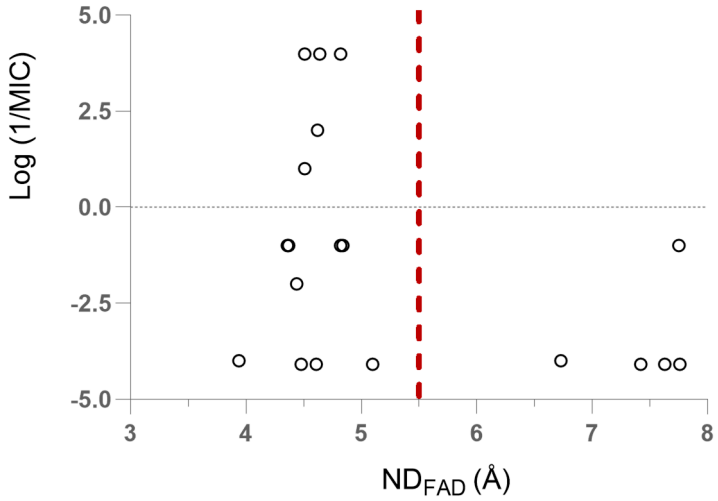

Figure 4. Relation between the activity of the compounds and the distance of the nitrogen atom of the nitro group to the nitrogen in the center portion of the isoalloxazine ring of the FAD cofactor. Distances above 5.5Å appear to lead to compounds with low activity.

Additionally, the type of interactions formed between each compound and the amino acid residues within the DprE1 pocket were identified using Protein-Ligand Interaction Profiler (PLIP) [23] (Figure 5).

Compound	MIC (μg/mL)	T60	L115	G117	H132	K134	S228	W230	Y314	L317	F320	E336	L363	V365	K367	N385	K418
c2	0,063					1	1	1		2	1			2			1
d2	0,063					1	1	1 1	1	2	1			1			1
d1	0,063					2	1		1	2	1			2			
c3	0,25					1				1	1			1	1		
a6	0,5					2		1		3	1			2			
a7	2					1	1	1 1		2	1			1			1
c4	2					1	1 2		1	3	1			1	1		
a5	2							2		1	1 1		1	2			
b3	2						1			1	1			1	1		
e1	2									1	1			1			
b2	4		1	1		1				2	1			1			
b1	16				1					1	1	1		1		1	
e2	16									1							1
c1	>16					1				1	1			2			
f1	>16	1															1
a1	>16									1	1						1
a3	>16									1 1							1
a8	>16									1	1			1			
a4	>16									1	1			1			1

Hidrophobic interactions
H-bonds
π-stacking
Salt bridge

Figure 5. Map of interactions between the best poses from the non-covalent docking of the compounds and DprE1.

Residues L134 , S228, and W230 are identified as critical interaction points for the most active compounds, whereas L317, F320, and V365 play a significant role for all investigated compounds.

The absence of a correlation between docking score and the activity in the noncovalent docking, combined with the inhibition mechanism involving a covalent bond formation between the inhibitor and protein, prompted the application of covalent docking for our compounds. In this covalent docking scenario, a correlation between the docking scores and compound activity was noted, with the most active compounds displaying higher docking scores. Furthermore, docking scores below 30 kcal/mol were found to correspond to compounds exhibiting lower activity, indicating a potential threshold for predicting compound efficacy. These docking scores are present in Table 2.

Considering the correlations observed between the bioactivity, quantified as log(1/MIC), and both lipophilicity (LogP) and covalent docking scores, we employed a multivariate linear regression with least squares optimization, to model these relationships and derived the equation: Bioactivity = 0.5958 * LogP + 0.07253 * Docking Score - 3.265. The resultant model exhibited a strong predictive

 doi:10.20944/preprints202403.0811.v1

capability, as evidenced by a correlation coefficient of 0.9061 (R = 0.9061, R^2 = 0.8211), between the predictors and the biological activity.

3. Discussion

In the first family of compounds (**a**), the linker consists of one heterocyclic structure containing a nitrogen atom and X can be CH, N, or O. When X is CH or N a terminal R can be present, being either an H, OH, Me_2, Benzyl or OPh-(4-OMe) as substituents. By analyzing the activities, we can see that there's two main sets of compounds in the family- one with moderate activities against Mtb (0,5 to 2 μg/mL), which have a terminal aromatic ring as a terminal group, and a second set of compounds that presents smaller groups in the terminal position, and that fail to have significant activity against Mtb (>16 μg/mL). This reveals that the aromaticity and/or lipophilicity that the addition of the aromatic moieties give to the compounds is very beneficial to their activity.

In family **b**, whose compounds have linear alkyl chains of variable size as linkers (2, 3 or 5 carbons) but no terminal group, there's an increase of activity as the linkers get bigger (and lipophilicity increases).

Family **c** consists of compounds where linear linkers with 2 or 5 carbons are connected to the terminal aromatic rings in 2 ways: ester or amide bonds. Between compounds **c1** and **c2** (esters) the only variation is the linker size (2 and 5 carbons, respectively), with both compounds having a (3,5-dinitrobenzoyl)oxy as a terminal group. This, however, had a big impact in the activity of the compounds, with the first compound not showing any meaningful activity and the second one showing activity comparable to INH and DNB1. We have no clear rationale to explain the difference in activity between **c1** and **c2**. This difference could be attributed in part to the lipophilicity of the compounds. Compound **c1**, with its 2 charged nitro groups on each end of the molecule and a short linker, may face some difficulty in passing through the lipophilic cell envelope of the mycobacteria. Compound **a8** may likely encounter a similar problem due to the presence of a positively charged quaternary amine in the terminal group's zone. Compounds **c2** and **c3** allow to compare the influence of the connection between the linker and the terminal group on the activity, with the ester bond being preferred over the amide bond. Finally, between the two diamides (**c3** and **c4**) the best one was the one with two nitroaromatic cores in the molecule (**c3**), despite **c4** being the most lipophilic of this family of compounds. However, this isn't surprising considering that **c3** is symmetrical and both extremities could covalently bond to DprE1, while only one could do it in the **c4** molecule.

The addition of the terminal aromatic ring to compounds **b2** and **b3** by an ether bond, to obtain **d1** and **d2** respectively, led to a significant increase in activity of the compounds. The difference in size of the linker didn't influence the activity, with both compounds showing equal antitubercular activities, which were comparable to INH and DNB1.

With the exception of compound **c1**, both the **c** and **d** families show a similar trend to the family **a**, where the addition of terminal aromatic moieties to the compounds is-beneficial to their activity, reinforcing the importance of this section of the molecule. This is also in accordance with the literature, which describes a preference for the substitution of a phenyl group over an alkyl group in the terminal group zone [12].

The simple addition of an aromatic ring isn't, however, enough to obtain good MIC values, with the linker also playing an important part in the activity of the compounds, since connecting an aromatic ring directly to the amide of the nitrobenzamide core (compound **f1**) resulted in an inactive compound. The cyclic linkers (family **a**) also seem to have lower activities than the linear linkers (families **c** and **d**), likely because of the added steric hindrance and/or the lower flexibility.

These observations are partially consistent with the literature, with the absence of the linker being described as detrimental to the activity [12], and the use of cyclic linkers or substituents higher than methyl in the first carbon of the linker near the amide, being also detrimental to the activity [11,12]. However, although some of the literature reports the increase of the linker size leading to decrease of potency [12], our compounds demonstrate that it can at least maintain the potency in the series created, since DNB1, **d1** and **d2** presented the comparable activities.

 doi:10.20944/preprints202403.0811.v1

Although there are other factors that also play a role in activity, lipophilicity is a property with a major impact in antitubercular activity. By calculating the lipophilicity of the compounds and plotting log P against their activity we can see that the more active compounds are, in general, more lipophilic than the less active ones (Figure 2). This isn't surprising given the characteristics of the cell wall of Mtb, which is effective at preventing the entry of the more polar compounds [24,25]. Thus, this is an important aspect to have in mind when further developing this class of inhibitors.

In the docking analysis with compounds **c2**, **d1** and **d2**, the optimal poses of these lead candidates are situated near FAD and cysteine, two critical sites for the inhibition mechanism of DprE1 by nitrobenzamides. Specifically, their proximity to FAD, essential for the initial step in this mechanism, suggests that the benzamides studied here likely employ a similar inhibition mechanism as other nitrobenzamides documented in scientific literature. This analysis may also shed light on the differing activities observed between compounds **e1** and **e2**. Unlike compounds **b1** and **b2**, the 'shorter' compound (implied to be **e1**) shows higher activity. This could be due to the positioning of **e1** in the protein's pocket, which aligns with that of the active compounds. In contrast, **e2** is oriented in reverse, with its 5,6-dihydro-4H-1,3-oxazine ring in a position akin to the nitroaromatic core of the active compounds. However, this observation should be interpreted with caution since some inactive compounds also share similar positioning to the active compounds. Thus, positioning alone may not be a reliable criterion for future development within this class of inhibitors. Nevertheless, plotting the distance from the nitro group to FAD against activity indicates that distances greater than 5.5 Å tend to be associated with compounds exhibiting lower activity. Additionally, the results from covalent docking, particularly scores below 30 kcal/mol, suggest lower activity. Moreover, a multivariate linear regression correlating the activity with both the LogP values, and the covalent docking score showed a good correlation coefficient ($r = 0.9061$). This regression model could be useful to predict the activity of future compounds based on their LogP values and covalent docking scores before experimental testing. These findings could be instrumental in guiding future synthetic modifications.

Additionally, looking at the list of interactions that the best poses of the compounds make with the receptor, some key interactions that are important for the activity of this class of compounds are revealed. In particular, the interaction with L134 appears in all of the active compounds, and some of the moderately active compounds, while it fails to appear in the compounds with low activity, and thus it may be an important interaction with the receptor. Interactions with S228 and W230 also appear more frequently in the more active compounds. Indeed, L134 and W230 have been reported as important residues that establish interactions with some of the DprE1 inhibitors, and S228, together with L134 and some other residues, form a hydrophilic cavity in the enzyme that is important to the affinity of the inhibitors [26]. Thus, for future development of the compounds, those that are able to make these interactions may have better activities. However, other interactions have also been reported and may be important for the activity [26], and thus may be worth considering as well, especially if the characteristics (e.g. size) of the compounds start to considerably deviate from the ones studied here.

4. Materials and Methods

Materials. Balanced salt solution, phosphate-buffered saline (PBS), Dulbecco's modified Eagle's medium (DMEM), and L-glutamine were purchased from Invitrogen. Sodium dodecyl sulphate (SDS), Triton X-100, 3,5-dinitrobenzoic acid, benzoic acid, piperidine, 4-benzylpiperidine, 4-hydroxypiperidine, piperazine, 4-benzylpiperazine, morpholine, 2-aminoethan-1-ol, 3-aminopropan-1-ol, 5-aminopentan-1-ol, 4-methoxyphenol, p-anisidine, triphenylphosphine, 1,1'-(azodicarbonyl)dipiperidine (ADDP), iodomethane, potassium carbonate, sodium iodide, sodium azide, thionyl chloride and trypan blue were purchased from Sigma-Aldrich Quimica SA. All solvents were used without purification as acquired from commercial sources. Middlebrook 7H10 agar was purchased from Difco (BD Difco, Franklin Lakes, NJ, USA). Microwell tissue culture plates were purchased from Nunc. All amides presented were synthesized according to the procedures described in this paper. Compounds were prepared in stock solutions of 40 mg/ml in dimethyl

 doi:10.20944/preprints202403.0811.v1

sulfoxide (DMSO – AppliChem Panreac). Isoniazid (Sigma-Aldrich) is a first line antibiotic against tuberculosis and was used as a positive control for M. tuberculosis killing.

Bacterial strains and cell lines. Bacteria broth culture medium Middlebrook 7H9 and solid culture medium Middlebrook 7H10 were purchased from Difco (BD Difco, Franklin Lakes, NJ, USA). All Mycobacterium spp. were cultivated in Middlebrook's 7H9 medium supplemented with 10% OADC (oleic acid, albumin, dextrose, catalase) enrichment (BD Difco, Franklin Lakes, NJ, USA), 0.02% glycerol, and 0.05% tyloxapol (Merck, KGaA) incubated at 37 °C until exponential growth phase was achieved. M. tuberculosis H37Rv (ATCC 27294), was used for MIC evaluation.

Synthesis. **1.Acyl chloride synthesis:** A solution of 3,5-dinitrobenzoic acid or benzoic acid in thionyl chloride (2 mL per mmol of acid) was refluxed for 12 h, leading to the formation of the respective acyl chloride. The excess thionyl chloride was removed by low pressure evaporation. The product was used without further purification.

2.General protocol to Amide synthesis: A solution of the appropriate acyl chloride (1 eq.) in ethyl acetate was added dropwise to a solution of corresponding amine (2 eq.) and K_2CO_3 (2 eq.) in ethyl acetate. When the reaction was complete (as assessed by TLC using hexane:ethyl acetate, 3:7 to 0:1 as eluent) the reaction mixture was filtered, and the filtrate washed successively with 10 mL of distilled water and with 15 mL of brine. The ethyl acetate solution was subsequently dried, and the solvent evaporated. The residue was purified by column chromatography (silica gel 60) using hexane: ethyl acetate, 1:1 to 2:8 as eluent.

3.General protocol to Mitsunobu reaction [18]**:**

A solution of the appropriate product (1 eq.), the respective phenol (1 eq.) and ADDP (2.5 eq.) in dichloromethane was placed under an atmosphere of nitrogen and for 10-15 min is purged with nitrogen. Then, to this mixture, a solution of PPh_3 (2.5 eq.) in dichloromethane was added dropwise, over a 2min period, and the reaction was stirred at room temperature for around 24 hours, all while keeping the reaction under a nitrogen atmosphere. After this, the DCM was evaporated, the mixture was dissolved in EtOAc and washed successively with 10 mL of distilled water and with 10 mL of brine. The ethyl acetate solution was subsequently dried, and the solvent evaporated. The residue was purified by column chromatography (silica gel 60) using hexane: ethyl acetate, 8:2 to 1:1 as eluent.

4.General protocol to the diamide formation:

For the synthesis of these compounds 4 different steps were required.

The first one was replacing the hydroxyl group with a chloro. For this, a solution of **b3** in a mixture of thionyl chloride, toluene and DMF (1/1/0.1, in a total volume of 3 mL per mmol of reactant), was refluxed for 12 h, leading to the formation of the desired product. The excess solvent mixture and thionyl chloride were removed by low pressure evaporation. Then, the mixture was dissolved in EtOAc and washed successively with 10 mL of distilled water and with 10 mL of brine. The ethyl acetate solution was subsequently dried, and the solvent evaporated. The residue was purified by column chromatography (silica gel 60) using hexane: ethyl acetate, 8:2 to 1:1 as eluent.

The second step was an S_N2 reaction to replace the chlorine with an azide. For this, a solution of the previous product, NaN_3 (3 eq.) and NaI (0,3 eq.) in MeCN were heated at 70ºC and stirred for 5 days. The MeCN was then removed by low pressure evaporation and the mixture was dissolved in EtOAc and washed successively with 10 mL of distilled water and with 10 mL of brine. The ethyl acetate solution was subsequently dried, and the solvent evaporated. The residue was purified by column chromatography (silica gel 60) using hexane: ethyl acetate, 8:2 to 1:1 as eluent.

The third step was the Staudinger reaction [20], to transform the azide into an amine. For this, the previous product and PPh_3 (2 eq.) were dissolved in THF, under a N_2 atmosphere, and was stirred for 24h. Then, a small quantity of distilled water is added to the mixture and the reaction is stirred for another 24h. The solvent is then evaporated, and the product used without further purification.

The fourth and final step consists on repeating the general protocol to Amide synthesis with amine product, utilizing both 3,5-dinitrobenzoyl chloride and benzoyl chloride, to yield **c3** and **c4**, respectively.

 doi:10.20944/preprints202403.0811.v1

All final compounds were characterized by ^{13}C NMR, ^{1}H NMR and MS. The purity of the compounds was further tested by TLC. Synthesis specifications, yields and structural data for compounds is available in the Supplementary Materials.

Compound characterization. ^{1}H NMR and ^{13}C NMR spectra were recorded on a Bruker Avance 400 spectrometer, in the indicated solvent; chemical shifts are reported in parts per million (ppm), relative to tetramethylsilane (TMS). The spectra were referenced to the solvent peak and coupling constants (J) are quoted in hertz (Hz). The mass spectra were recorded on a AcquityTM triple quadrupole spectrometer (ESI); compounds were analysed in solution of MeCN, and m/z values are reported in Daltons.

Determination of the Minimum Inhibitory Concentration (MIC) and Minimum Bactericidal Concentrations (MBC): The MICs were determined by the broth microdilution method in 96-well plates. Briefly, M. tuberculosis bacterial cultures in exponential growth phase were collected by centrifugation, washed with PBS and re-suspended in fresh culture medium. Clumps of bacteria were removed by ultrasonic treatment of the bacteria suspension in an ultrasonic water bath for 5 min followed by a low-speed centrifugation (500 x g) for 2 min. Single cell suspension was verified by microscopy. The microplates containing a bacterial suspension corresponding to approximately 105 colony-forming units per ml were incubated with the selected concentrations of the compounds. Every other day, the optical density of the wells was measured in a Tecan M200 spectrophotometer, following 30 s of orbital agitation. These values were used to produce the growth curves. At the 10th day of incubation, the MIC was determined, corresponding to the concentration with no visible turbidity. Optical density measurements were taken until the 15th day of incubation. The MBC values were determined using an established methodology[27]. Briefly, following MIC determination, the bacterial samples were recovered from the MIC test microplates and plated in 7H10 + OADC solid medium. The MBC was determined following 3 weeks of incubation, corresponding to the concentration of compound that produced no colonies on the solid medium. Bacteria treated with DMSO solvent at the same proportions as present during the compound tests were used as a control. Isoniazid was used as a positive control for bacteria killing and assay validation following EUCAST guidelines (MIC = [0.03, 0.12] μg/mL). All MIC and MBC results presented comprise the mode value of a minimum of triplicate experiments.

LogP determination: The predicted LogP values were calculated using SwissADME [28] and correspond to the average of the values from iLOGP, XLOGP3, WLOGP and MLOGP.

Molecular docking: The receptor structure was retrieved from the RCSB Protein Data Bank entry 4FDN (PDB: 4FDN), which corresponds to the crystal structure of M. tuberculosis DprE1 in complex with the covalent inhibitor CT325. Initially, all water molecules and ligands, except for water molecule 1035, were removed. The protein's structure was then prepared using the Molecular Operating Environment (MOE2020) software. Within this environment, missing loops were built using the "Build Loop" tool, structural errors corrected, and charges and protonation states assigned via the "Protonate 3D" tool, applying standard conditions (pH = 7 and T = 300 K). The refined structure was saved in mol2 format.

The 3D models of the compounds under study were prepared with MOE. The SMILES strings of the compounds were obtained and then input to MOE's database and processed sequentially through the "Wash", "Partial Charges", and "Energy Minimization" steps using default parameters before being saved as mol2 files.

Molecular docking simulations were performed using GOLD software [22], employing the default values and using the ASP scoring function. A search space of 20$Å^3$, entered on the ligand's position in the crystallographic structure, was defined, and each ligand was docked 100 times. Poses were ranked according to the scoring functions, selecting the lowest-energy conformation for each compound. The coordinates of the top pose for each compound were used to calculate the distance from the nitrogen atom of their nitro groups to two critical receptor atoms: the sulfur atom in Cys387 and the nitrogen atom in the central part of the isoalloxazine ring of the FAD cofactor within the binding pocket. Covalent docking was also conducted using the ASP scoring function, for which compounds were modified by removing an oxygen atom from one of the nitro groups, and the

 doi:10.20944/preprints202403.0811.v1

nitrogen of this modified nitro group and the sulfur of Cys387 were designated for covalent bond formation.

The Protein-Ligand Interaction Profiler (PLIP) was used to identify the interactions between the DprE1 structure and the best poses from the noncovalent docking of each compound, providing comprehensive insights into the binding mechanisms [23].

5. Conclusions

The synthesis of a library of dinitrobenzamides allowed to enhance the understanding of the role of the linker and the terminal group in the antitubercular activity of the compounds. The results here discussed show that high antitubercular activities are obtained when an aromatic terminal group is present, with linear linkers being more favourable than cyclic linkers. They also show the importance of the linker in the activity since its omission led to an inactive compound. Another characteristic that has a significant effect in the activity is the lipophilicity of the compounds. Computational studies indicate that the most active compounds are placed in the expected area according to the mechanism of inhibition. Nevertheless, the methodology lacks the discriminatory capability to fully distinguish between active and non-active compounds. Still, looking at ND_{FAD}, the covalent docking score and the interactions established could allow us to filter out some of the inactive compounds. The regression model could also be useful to predict the activity of future compounds based on their covalent docking score and LogP. Among the synthesized compounds, those belonging to the **d** family and compound **c1** have demonstrated significant potential, exhibiting activities capable of rivalling that of Isoniazid and also retaining the activity level observed in other inhibitors within this class, like DNB1. Thus, these compounds stand as promising candidates to be lead molecules in the future development of nitrobenzamides. Additionally, insights into the required lipophilicity and docking "benchmarks" for prospective compounds have been revealed, serving as valuable guidelines to prioritize synthesis efforts effectively, and the synthetic pathways utilized can be easily adapted in future synthetic endeavours.

Supplementary Materials: The following supporting information can be downloaded at the website of this paper posted on Preprints.org, Annex 1—synthesis details and structural characterization.

Author Contributions: T.D.: investigation (chemistry and docking), methodology, writing - original draft, conceptualization; J.P.: investigation (chemistry, microbiology and docking), methodology, writing—review and editing, supervision; D.P.: investigation (microbiology); F.E.: investigation (docking); R.G.: supervision (docking), methodology, resources; E.A.: supervision (microbiology), resources; L.C.: conceptualization, methodology, writing—review and editing, supervision, project administration, funding acquisition. All authors have read and agreed to the published version of the manuscript.

Funding: This research was funded by Fundação para a Ciência e Tecnologia (FCT), grant number EXPL/SAU-INF/1097/2021. It also received financial support from FCT (via Imed ULisboa) from projects UIDB/04138/2020 and UIDP/04138/2020.

Institutional Review Board Statement: Not applicable.

Informed Consent Statement: Not applicable.

Data Availability Statement: Data available within the article.

Conflicts of Interest: The authors declare no conflict of interest. The funders had no role in the design of the study; in the collection, analyses, or interpretation of data; in the writing of the manuscript, or in the decision to publish the results.

References

1. *Global tuberculosis report 2023*. 2023.
2. M. de Martino, L. Lodi, L. Galli, and E. Chiappini, "Immune Response to Mycobacterium tuberculosis: A Narrative Review," *Front Pediatr*, vol. 7, Aug. 2019. https://doi.org/10.3389/fped.2019.00350.

3. N. Blondiaux *et al.*, "Reversion of antibiotic resistance in Mycobacterium tuberculosis by spiroisoxazoline SMARt-420," *Science (1979)*, vol. 355, no. 6330, 2017. https://doi.org/10.1126/science.aag1006.
4. F. Liang, R. Tantan, Z. Peize, and L. Shuihua, "Interpretation of WHO consolidated guidelines on tuberculosis, Module 4 : treatment-drug-resistant tuberculosis treatment, 2022 update," *Chinese Journal of Antituberculosis*, vol. 45, no. 4, 2023. https://doi.org/10.19982/j.issn.1000-6621.20220523.
5. G. S. Shetye, S. G. Franzblau, and S. Cho, "New tuberculosis drug targets, their inhibitors, and potential therapeutic impact," *Translational Research*, vol. 220. 2020. https://doi.org/10.1016/j.trsl.2020.03.007.
6. G. Manina, M. R. Pasca, S. Buroni, E. De Rossi, and G. Riccardi, "Decaprenylphosphoryl-β-D-Ribose 2-Epimerase from Mycobacterium tuberculosis is a Magic Drug Target," *Curr Med Chem*, vol. 17, no. 27, 2010. https://doi.org/10.2174/092986710791959693.
7. J. Mi, W. Gong, X. Wu, and A. M. Al Attar, "Advances in Key Drug Target Identification and New Drug Development for Tuberculosis," *BioMed Research International*, vol. 2022. 2022. https://doi.org/10.1155/2022/5099312.
8. A. Richter *et al.*, "Novel insight into the reaction of nitro, nitroso and hydroxylamino benzothiazinones and of benzoxacinones with Mycobacterium tuberculosis DprE1," *Sci Rep*, vol. 8, no. 1, 2018. https://doi.org/10.1038/s41598-018-31316-6.
9. J. Neres *et al.*, "Structural basis for benzothiazinone-mediated killing of Mycobacterium tuberculosis," *Sci Transl Med*, vol. 4, no. 150, 2012. https://doi.org/10.1126/scitranslmed.3004395.
10. V. Makarov *et al.*, "Benzothiazinones Kill Mycobacterium tuberculosis by blocking Arabinan synthesis," *Science (1979)*, vol. 324, no. 5928, 2009. https://doi.org/10.1126/science.1171583.
11. T. Christophe *et al.*, "High content screening identifies decaprenyl-phosphoribose 2′ epimerase as a target for intracellular antimycobacterial inhibitors," *PLoS Pathog*, vol. 5, no. 10, 2009. https://doi.org/10.1371/journal.ppat.1000645.
12. G. Munagala *et al.*, "Synthesis and biological evaluation of substituted N-alkylphenyl-3,5-dinitrobenzamide analogs as anti-TB agents," *Medchemcomm*, vol. 5, no. 4, pp. 521–527, 2014. https://doi.org/10.1039/c3md00366c.
13. A. Wang *et al.*, "Design, synthesis and antimycobacterial activity of 3,5-dinitrobenzamide derivatives containing fused ring moieties," *Bioorg Med Chem Lett*, vol. 28, no. 17, pp. 2945–2948, Sep. 2018. https://doi.org/10.1016/j.bmcl.2018.07.005.
14. H. Wang *et al.*, "Design, synthesis and antimycobacterial activity of novel nitrobenzamide derivatives," *Chinese Chemical Letters*, vol. 30, no. 2, pp. 413–416, Feb. 2019. https://doi.org/10.1016/j.cclet.2018.08.005.
15. L. Li *et al.*, "Identification of N-Benzyl 3,5-Dinitrobenzamides Derived from PBTZ169 as Antitubercular Agents," *ACS Med Chem Lett*, vol. 9, no. 7, pp. 741–745, Jul. 2018. https://doi.org/10.1021/acsmedchemlett.8b00177.
16. O. Antoniuk, "Pró-fármacos contendo álcoois de cadeia longa para tratamento da tuberculose. Investigação do mecanismo de ação," Faculdade de Farmácia da Universidade de Lisboa, Lisbon, 2022.
17. J. P. Pais *et al.*, "Benzoic Acid Derivatives as Prodrugs for the Treatment of Tuberculosis," *Pharmaceuticals*, vol. 15, no. 9, 2022. https://doi.org/10.3390/ph15091118.
18. P. S. Humphries, Q. Q. T. Do, and D. M. Wilhite, "ADDP and PS-PPh3: An efficient Mitsunobu protocol for the preparation of pyridine ether PPAR agonists," *Beilstein Journal of Organic Chemistry*, vol. 2, 2006. https://doi.org/10.1186/1860-5397-2-21.
19. M. Brandstätter, F. Roth, and N. W. Luedtke, "Synthesis of 2-oxazolines by in situ desilylation and cyclodehydration of β-hydroxyamides," *Journal of Organic Chemistry*, vol. 80, no. 1, 2015. https://doi.org/10.1021/jo5016695.
20. S. Liu and K. J. Edgar, "Staudinger reactions for selective functionalization of polysaccharides: A review," *Biomacromolecules*, vol. 16, no. 9. 2015. https://doi.org/10.1021/acs.biomac.5b00855.
21. S. M. Batt *et al.*, "Structural basis of inhibition of Mycobacterium tuberculosis DprE1 by benzothiazinone inhibitors," *Proc Natl Acad Sci U S A*, vol. 109, no. 28, 2012. https://doi.org/10.1073/pnas.1205735109.
22. G. Jones, P. Willett, R. C. Glen, A. R. Leach, and R. Taylor, "Development and validation of a genetic algorithm for flexible docking," *J Mol Biol*, vol. 267, no. 3, 1997. https://doi.org/10.1006/jmbi.1996.0897.
23. M. F. Adasme *et al.*, "PLIP 2021: Expanding the scope of the protein-ligand interaction profiler to DNA and RNA," *Nucleic Acids Res*, vol. 49, no. W1, 2021. https://doi.org/10.1093/nar/gkab294.
24. P. J. Brennan and H. Nikaido, "The envelope of mycobacteria," *Annual Review of Biochemistry*, vol. 64. 1995. https://doi.org/10.1146/annurev.bi.64.070195.000333.
25. R. C. Goldman, "Why are membrane targets discovered by phenotypic screens and genome sequencing in Mycobacterium tuberculosis?," *Tuberculosis*, vol. 93, no. 6. 2013. https://doi.org/10.1016/j.tube.2013.09.003.
26. S. Yadav, A. Soni, O. Tanwar, R. Bhadane, G. S. Besra, and N. Kawathekar, "DprE1 Inhibitors: Enduring Aspirations for Future Antituberculosis Drug Discovery," *ChemMedChem*, vol. 18, no. 16. 2023. https://doi.org/10.1002/cmdc.202300099.

 doi:10.20944/preprints202403.0811.v1

27. N. C. D. S. Santos *et al.*, "Minimum Bactericidal Concentration Techniques in Mycobacterium tuberculosis: A Systematic Review," *Microbial Drug Resistance*, vol. 26, no. 7. 2020. https://doi.org/10.1089/mdr.2019.0191.
28. A. Daina, O. Michielin, and V. Zoete, "SwissADME: A free web tool to evaluate pharmacokinetics, drug-likeness and medicinal chemistry friendliness of small molecules," *Sci Rep*, vol. 7, 2017. https://doi.org/10.1038/srep42717.